Construction and Building Materials 309 (2021) 124967

Contents lists available at ScienceDirect

Construction and Building Materials

journal homepage: www.elsevier.com/locate/conbuildmat

Influence of high temperatures on the bond between carbon Fibre-Reinforced polymer bars and concrete

Fernando Cos-Gayón López *, Javier Benlloch Marco, Víctor Calvet Rodríguez

Centro de Investigación de Tecnología de la Edificación, CITE, Universitat Politècnica de València, Spain

ARTICLE INFO

Keywords:
Bond strength
CFRP
Temperature
Stress
Deformation

ABSTRACT

The effect of corrosion on reinforced concrete structures can lead to significant economic losses. Therefore, steel bars used in the concrete structures must be replaced with a different material that can withstand water contact without causing corrosion and can ensure the safe operation of the structure during its lifespan, even in adverse weather. Carbon-fibre-reinforced polymer (CFRP) bars are one of the materials that can replace steel bars and they have already been applied as a substitute previously. This study analyses the bonding of these bars with concrete at high temperatures and for longer time periods. It presents an experimental plan that involves a series of pullout trials at different ages, days, and thermal conditions in CFRP rods either treated with ribbed steel bars or that underwent sand-ribbed surface treatment. Some compression tests for each mixture were performed at the same ages and temperatures as the experimental plan in pullout to determine the influence of high temperatures on concrete. The study completed with some complementary tests on the CFRP rods using optical microscopy, scanning electron microscopy (SEM), and atomic force microscopy (AFM), from the evaluated pullout samples. The high temperature significantly affected the ribbed CFRP bars by diminishing their bond stress and did not affect the sanded CFRP bars. This uneven behaviour and the influence of high temperature on concrete resistance at the age of 180 d is justified.

1. Introduction

Steel is the most used material in reinforced concrete as it serves many purposes. Its excellent tensile stress and compatibility with concrete are ideal for structural calculations. Although reinforced concrete can be exposed to adverse environments such as chloride concentrations (marine structures and ice-melting salts), variations in temperature and humidity may cause its structural deterioration.

The repair and maintenance cost of existing infrastructure around the world is estimated over 100 billion euros [1,2]. A significant proportion of this expense is used to address the durability issues in concrete structures.

The alkaline environment of concrete usually provides necessary protection for reinforcement steel over conventional environments. Nevertheless, environmental wear is unavoidable, eventually decreasing the alkalinity of concrete coating, which leads to the corrosion and deterioration of reinforced concrete that facilitates shedding and increases damage [3].

Fibre-Reinforced Polymer (FRP) rods, owing to their characteristics, emerged into the global market in the 1990 s as a resolution to the corrosion issue [4]. The advantages of FRPs include a high resistance against corrosion, high strength-to-weight ratio (10–15 times greater than steel), excellent stress characteristics (approximately three times higher than steel), electromagnetic neutrality, and easy commissioning work, which reduces building cost. However, their disadvantages include high cost, low ductility with an easy rupture, and low shearing resistance (caused by the poor mechanical properties of the matrix, such as fast and severe bonding loss or resistance and rigidity at high temperatures).

Numerous studies have been conducted on fibre-reinforced polymers [5–23]. Benmokrane et al. [24] found that the bond strength of the steel bars with sand-coated CFRP and ribbed CFRP bars was same as concrete. Moon et al. [25] found that increasing the quantity of milled glass fibre improved the connections between the core and rib sections of the GFRP rebars. Even though these studies do not focus on bond mechanisms and high temperature influence on reinforced concrete with this material, falling for a behaviour analysis of a few hours of exposure [5,26–29]. Achillides [5] obtained 2.5–5.0 mPa of bond tension in corrugated CFRP

* Corresponding author.
E-mail addresses: fcosgay@csa.upv.es (F. Cos-Gayón López), jabenllo@csa.upv.es (J. Benlloch Marco), vccalrod@csa.upv.es (V. Calvet Rodríguez).

https://doi.org/10.1016/j.conbuildmat.2021.124967
Received 8 December 2019; Received in revised form 30 May 2021; Accepted 16 September 2021
Available online 6 October 2021

Table 1
Data from the pullout test in steel bars, stress with slippings of 0′01 mm, 0′1 mm, and 1 mm, slipping on a non-stressed end (δ_{ENT}), stressed end (δ_T), maximum stress, and characteristic bond strength.

BAR TYPE	TIME (d)	TEMPERATURE (°C)	SPECIMENS	LOT	$\tau_{med.}$ 0.01 mm (MPa)	$\tau_{med.}$ 0.1 mm (MPa).	$\tau_{med.}$ 1 mm (MPa)	$\tau_{med.}$ (MPa)	δ_{ENT} (mm)	δ_{ET} (mm)	**τ máx (MPa)**	**τmed Normal. (MPa)**	FAILURE MODE
FCC12	28	20 °C	A	3	1,4404	3,0729	14,3952	6,3028	1,2150	1,8490	8,92	3,15	RA
			B	3	4,5101	8,1235	20,3269	10,9868	1,4883	3,0574			RC
			C	3	1,9547	6,4558	19,9572	9,4559	1,2010	1,7393			RC
		50 °C	A	3	2,0349	4,5910	12,8345	6,4868	1,2798	1,6842	7,57	2,49	RA
			B	3	2,7434	8,3281	15,9394	9,0036	1,3915	2,1688			RA
			C	3	2,5742	5,8673	13,1857	7,2091	1,3460	1,8173			RA
		80 °C	A	3	0,1149	4,2889	13,7806	6,0615	1,2777	2,1392	6,93	2,52	RA
			B	3	0,7213	5,7910	11,1497	5,8873	1,2690	1,8926			RA
			C	3	1,9243	8,5794	16,0112	8,8383	1,0368	2,4716			RA
	60	20 °C	A	6	0,7922	3,5183	6,5807	3,6304	0,2189	0,4414	8,64	3,14	RC
			B	6	0,9928	5,7584	19,6156	8,7889	1,1983	2,1547			RA
			C	6	1,1714	4,7623	19,5271	8,4869	1,4580	2,8321			RA
		50 °C	A	6	0,7169	4,0559	16,3815	7,0514	1,0186	1,7908	7,86	2,96	RA
			B	6	1,2051	7,1446	18,0511	8,8003	0,9562	1,5560			RA
			C	6	1,5387	5,5548	16,0686	7,7207	0,9515	2,5700			RA
		80 °C	A	6	0,1655	6,9444	16,1725	7,7608	0,7684	1,9023	7,89	2,86	RA
			B	6	1,0388	5,5925	13,0635	6,5649	1,1298	1,9336			RA
			C	6	1,6307	8,7157	17,6576	9,3347	0,9736	1,8376			RA
	180	20 °C	A	9	2,4031	8,4199	16,0442	8,9557	0,7891	1,5918	10,98	2,88	RA
			B	9	5,5960	12,4655	19,3312	12,4642	0,7577	1,3039			RA
			C	9	2,2322	9,2254	23,0670	11,5082	0,9679	1,8068			RA
		50 °C	A	9	1,1964	4,5904	13,6843	6,4904	2,1051	3,2999	8,60	3,07	RA
			B	9	1,0492	8,0854	21,9242	10,3529	0,9713	1,9297			RA
			C	9	1,0038	6,8376	19,0462	8,9625	0,8849	1,8586			RA
		80 °C	A	9	0,4522	4,4716	16,3209	7,0816	0,8606	1,5053	7,71	2,76	RA
			B	9	1,4953	8,4944	18,2342	9,4080	0,7355	0,9146			RA
			C	9	1,2185	4,7282	13,9701	6,6389	1,0170	1,4719			RA

Table 2
Data from the pullout test in sand CFRP, stress with slippings of 0′01 mm, 0′1 mm, and 1 mm, slipping on a non-stressed end (δ_{ENT}), stressed end (δ_T), maximum stress, and characteristic bond strength.

BAR TYPE	TIME (d)	TEMPERATURE (°C)	SPECIMENS	LOT	$\tau_{med.}$ 0.01 mm (MPa)	$\tau_{med.}$ 0.1 mm (MPa)	$\tau_{med.}$ 1 mm (MPa)	$\tau_{med.}$ (MPa)	δ_{ENT} (mm)	δ_{ET} (mm)	**τ máx (MPa)**	**τmed Normal. (MPa)**	FAILURE MODE
FCA14	28	20 °C	A	2	4,1745	8,9725	10,5903	7,9124	0,4989	0,8040	5,79	1,71	RA
			B	2	2,2953	3,5733	10,6450	5,5045	1,3019	1,4847			RA
			C	2	1,4290	2,2624	8,2090	3,9668	1,7540	2,5145			RA
		50 °C	A	2	0,0466	8,9784	9,2277	6,0842	0,1721	0,5862	7,01	1,62	RA
			B	2	3,7625	7,9772	8,1028	6,6142	0,1861	13,4350			RA
			C	2	6,6023	8,9157	9,4719	8,3300	0.2466	0,3696			RA
		80 °C	A	2	4,3917	7,5874	8,0096	6,6629	0,2501	0,7183	7,68	1,76	RA
			B	2	3,4897	7,2035	8,7306	6,4746	0,4535	0,9026			RA
			C	2	7,5433	10,6457	11,5499	9,9130	0,3498	0,8087			RA
	60	20 °C	A	5	0,6290	4,6805	7,2377	4,1824	0,2688	0,7119	7,93	1,68	RA
			B	5	3,3330	5,2580	5,5589	4,7166	0,3155	0,5790			RA
			C	5	1,6804	4,4499	4,6151	3,5818	0,0650	0,1966			RA
		50 °C	A	5	2,7257	6,4364	7,5223	5,5615	0,3945	0,7723	6,22	1,46	RA
			B	5	4,0269	7,8863	8,0462	6,6531	0,1716	0,5291			RA
			C	5	3,1110	7,0290	9,1536	6,4312	0,4186	0,7338			RA
		80 °C	A	5	1,0883	1,8188	9,3990	4,1020	1,0300	1,2221	4,89	1,64	RA
			B	5	2,0974	6,0554	8,7549	5,6359	0,4491	0,6597			RA
			C	5	1,8615	5,7485	7,2135	4,9412	0,3430	1,4961			RA
	180	20 °C	A	8	10,5444	14,3004	14,3500	13,0649	0,0633	0,5194	12,22	1,81	RA
			B	8	12,4235	12,4495	12,4495	12,4408	0,0141	0,6514			RA
			C	8	8,7783	12,0890	12,6400	11,1691	0,1173	0,6234			RA
		50 °C	A	8	6,0481	17,8290	20,6181	14,8317	0,3853	1,4691	15,21	3,07	RA
			B	8	11,0384	18,9718	19,6426	16,5509	0,2616	0,9643			RA
			C	8	7,9556	17,2268	17,5877	14,2567	0,1933	0,6652			RA
		80 °C	A	8	15,3466	19,9169	20,2013	18,4883	0,1847	0,6042	15,79	3,25	RC
			B	8	6,3368	17,2248	18,9765	14,1794	0,2305	0,8691			RA
			C	8	8,7539	16,8163	18,5076	14,6926	0,3755	1,5928			RC

bars, and Aiello [26] obtained 3.5–12.0 mPa in sand coated bars, in the initial stage. Achillides and Pilakoutas [29] observed that, in advanced stages of tension, there was no slippage at the untensioned end. Tepfers [17] and Achillides and Pilakoutas[29] found that the mechanical wedging stresses were balanced by an "α" angle that depended on the elastic modulus and surface geometry of the Carbon-fibre-reinforced polymer (CFRP) bar as well as the shear resistance of concrete, owing to the reaction of concrete that surrounded them. In CFRP corrugated bars, failure depends on the relationship between the concrete tensile strength and shear strength of the corrugations [29]. Various studies on

Table 3
Data from the pullout test in ribbed CFRP, stress with slippings of 0′01 mm, 0′1 mm, and 1 mm, slipping on a non-stressed end (δ_{ENT}), stressed end (δ_T), maximum stress, and characteristic bond strength.

Bar type	Time (d)	Temperature (°C)	Specimens	LOT	$\tau_{med.}$ 0.01 mm (MPa)	$\tau_{med.}$ 0.1 mm (MPa)	$\tau_{med.}$ 1 mm (MPa)	$\tau_{med.}$ (MPa)	δ_{ENT} (mm)	δ_{ET} (mm)	**τ máx (MPa)**	**τmed Normal. (MPa)**	FAILURE MODE
ACC12	28	20 °C	A	1	6,2251	9,6486	14,3470	10,0736	1,0624	1,6636	12,73	2,23	PO
			B	1	2,9019	4,5177	13,4585	6,9594	1,3019	1,5066			PO
			C	1	1,8067	2,8603	10,3788	5,0153	1,7540	2,5285			PO
		50 °C	A	1	2,1965	4,7502	10,3116	5,7528	1,1548	1,7716	10,78	1,96	PO
			B	1	1,5801	5,1643	10,1491	5,6312	0,6644	1,0139			PO
			C	1	1,7929	5,2281	11,8848	6,3019	1,0623	0,9563			PO
		80 °C	A	1	2,4272	5,5527	11,0061	6,3287	0,7648	1,6568	11,00	2,09	PO
			B	1	2,6798	5,8753	11,2360	6,5970	0,9067	–			PO
			C	1	3,2474	7,1443	10,7641	7,0519	1,0645	1,1801			PO
	60	20 °C	A	4	4,7727	10,7063	14,6735	10,0508	0,8709	1,3448	16,04	2,72	PO
			B	4	4,3182	11,0710	16,9031	10,7641	1,1785	2,2769			PO
			C	4	4,6697	10,6044	16,5525	10,6089	0,8034	1,4629			PO
		50 °C	A	4	3,9980	9,6791	14,9396	9,5389	0,6981	1,5160	14,76	2,61	PO
			B	4	3,1002	8,5185	14,0138	8,5442	0,8565	2,4824			PO
			C	4	2,1823	7,5608	15,3394	8,3608	1,1389	2,1737			PO
		80 °C	A	4	4,7894	10,2571	17,3628	10,8031	0,9028	2,1107	16,87	3,11	PO
			B	4	0,7978	2,7310	16,2946	6,6078	1,4068	2,1061			PO
			C	4	9,1929	9,9429	16,9450	12,0269	1,3936	–			PO
	180	20 °C	A	7	6,1881	16,8887	25,4611	16,1793	1,4183	–	27,64	4,04	PO
			B	7	8,6277	19,7370	28,4025	18,9224	1,5031	16,8438			PO
			C	7	9,6457	24,4049	29,0645	21,0384	1,5185	18,0985			PO
		50 °C	A	7	4,7293	17,0044	26,7895	16,1744	1,1567	11,1280	27,10	4,48	PO
			B	7	3,9561	14,3601	26,5189	14,9450	1,0844	–			PO
			C	7	8,8704	18,9424	27,8200	18,5443	1,2185	12,0108			PO
		80 °C	A	7	9,8239	19,1243	25,9217	18,2900	0,9424	8,2845	24,99	4,30	PO
			B	7	8,6340	16,6614	26,2554	17,1836	1,0471	7,5769			PO
			C	7	4,5315	10,5620	22,8039	12,6325	1,2627	–			PO

Fig. 1. Sand CFRP bar d14 (up), steel d12 (middle), ribbed CFRP d12 (down).

adherence behaviour [4,6,19,27,29–33] found that, the adherence behaviour of CFRP or Glass-fibre-reinforced polymer (GFRP) bars with concrete significantly depends on the tensile and shear strength of CFRP bars, the compressive strength of concrete, the diameter and surface geometry of the bar, confining pressure, anchor length, coating thickness, and bar position relative to the concrete and temperature. Furthermore, Benmokrane et al. [31] found that the distribution of bond stress along the embedment length of GFRP bars is nonlinear. Few studies have been conducted to investigate the effect of CFRPs on high-strength concrete (HSC) [5,4]. Bank et al. [34] showed a good correlation between the material degradation as well as the decrease in bond strength and stiffness of the FRP bars. Rafi et al. [35] found a narrow crack width using beams, exhibiting a good mechanical bond between the CFRP bars and the surrounding concrete.

Studies on the influence of temperature on the bond behaviour of CFRP bars with concrete have been carried out, especially, in ranges close to the glass transition temperature (Tg) of the resin, as it significantly modifies the bar properties. The mechanical properties of the polymer begin to reduce at a temperature close to its glass transition temperature, and the polymer cannot effectively transfer the stresses from the concrete to the fibres, with a considerable reduction in bond strength [36]. Thermosetting polymers (e.g. vinyl ester and polyester) have glass transition temperatures in the range of 60–130 °C, while high-performance inorganic and organic fibres, such as glass, carbon, and aramid fibres, exhibit good mechanical property retention at elevated temperatures (up to 250 °C) [37]. [38,39] observed that, at a temperature of 125 °C, the bond strength reduced by almost 50% of that at room temperature [5]. Yu and Kodur, observed 80% bond loss in their tests when the temperature increased from 20 to 200 °C. There are a few studies on temperatures below 100 °C that can be usual in-service

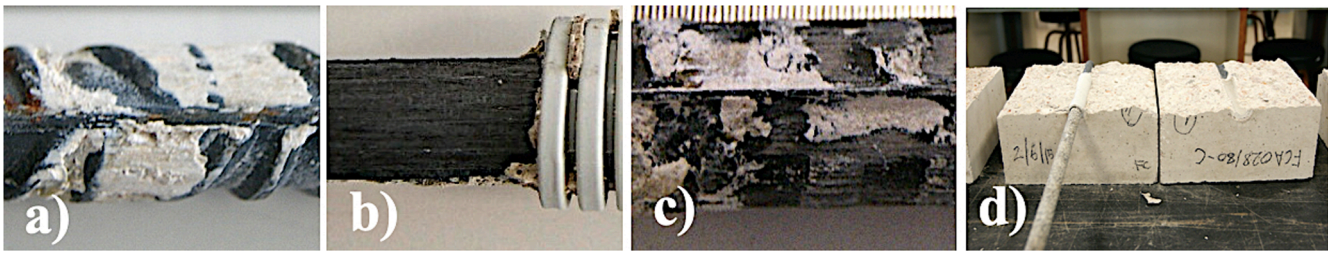

Fig. 2. Kinds of rupture: a) PO, b) RA, c) and RC. d) Test piece used in pullout and analysed.

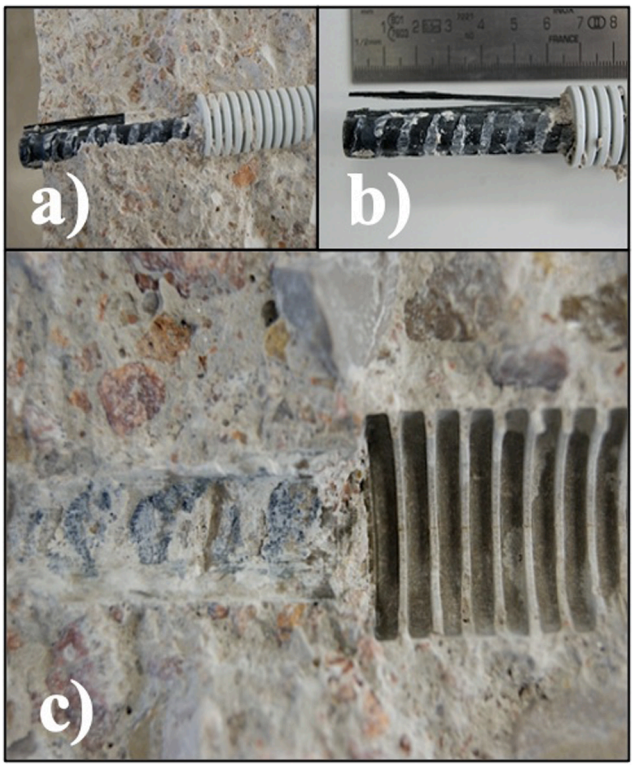

Fig. 3. Pullout ribbed CFRP bar test sample. Tested at 28 d of age and 20 °C. a) Bonding length of the tested concrete bar. b) Ribbed marks have completely disappeared on the bonding length. c) Corrugations embedded in the tested concrete after the trial.

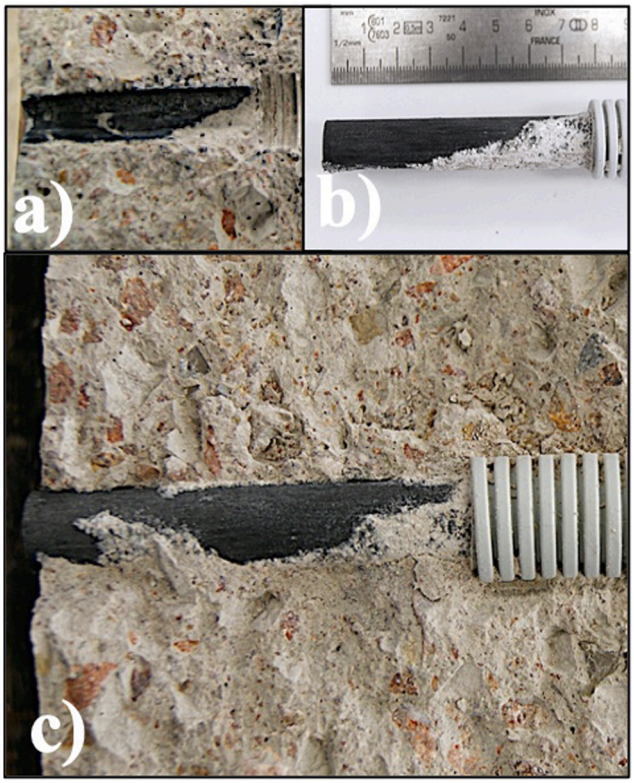

Fig. 4. Pullout sand CFP bar test sample. Tested at 180 d of age and 80 °C. a) Granular coating bonded to concrete and shredded from the nucleus of the bar. b) Bonding length without covering that ended up bonded in concrete. c) Tested concrete bar displaying areas without granular coating.

conditions. A structural element exposed to the sun, in the Mediterranean climate zone, can experience a temperature higher than 80 °C and an intensity higher than 600 W/m^2 in summer, following the Newton's law of cooling and the law of heat conduction (Fourier's law), without entering extreme situations such as desserts. Owing to various transverse coefficients of thermal expansion of the FRP bars and concrete, a high radial pressure is created, causing rupture stresses within the concrete. When the rupture stresses are equivalent to the tensile strength of concrete (fct), microcracks occur and weaken the links [40]. The bond strength between the FRP bars and concrete is severely affected, even at relatively low temperatures. A rapid loss in the bond strength was observed (up to 60% of room temperature) at 100 °C [41]. Davalos [11] found 20–30% reduction in the bond stress at a temperature of 80 °C compared to that at 20 °C. Bank et al. [34] observed that the FRP bars at a temperature of 80 °C showed minimum material degradation when compared to identical control bars held at room temperature (20–22 °C). Masmoudi et al. [42] observed that the ratio of concrete cover thickness to bar diameter must be greater than 1.6 to avoid the cracking of concrete under high temperatures up to 80 °C. Katz et al. [37] found that sand-coated or helix-bonded FRP bars develop a higher residual bonding characteristic at 200 °C compared to other bars with mechanical anchoring. [28] proposed a model of residual tensile strength for FRP bars with temperatures below 100 °C for a short exposure time of 4 h. [37] tested specimens at a high heating rate of ± 5 °C/min, simulating the conditions during a fire. Other authors, Rafi et al. [43], also studied the behaviour of CFRPs via beams subjected to a standard heating curve during a fire. Rafi et al. [43] found no signs of damage or splitting cracks owing to the difference in the transverse coefficient of thermal expansion of the CFRP bars and concrete.

This research is an advancement towards studying the effects of climatic conditions on the bond between the CFRP bars and concrete over time, from a few hours to over six months in a climate chamber.

2. Experimental plan

Multiple variables affect the bond between the CFRP bars and concrete resulting in the highest bond stress and mode of failure. However, there are a few studies on the effect of the behaviour of CFRP bars on bonding with concrete at high temperatures with the glass transition temperature (Tg). The objective of this research is to examine the thermal stages from 50 to 80 °C and their influence on various types of bars.

The criteria used to determine the bonding behaviour are essential for further analysis and discussion. The pullout method was selected owing to the discrepancy of the topic, which has been specified in the norm ACI 440-3R-12 because of the lack of uniformity [27].

It is interesting to compare the obtained results of the CFRP bars with the steel ones. The CFRP bars were manufactured to fix the durability and maintenance issues of the reinforced concrete with steel (justifying the introduction of CFRP concrete bars over the calculus of the structural design) [5,19,27].

Superficial treatment was conducted over ribbed and sanded bars to actively collaborate the mobilisation of bonding.

Optical microscopy tests such as Scanning Electron Microscopy (SEM) and Atomic Force Microscopy (AFM) were conducted to analyse the effect of high temperatures on the CFRP bars before and after the pullout tests.

Eighty-one pullout tests were conducted corresponding to three samples of each bar (sanded CFRP, ribbed CFRP, and steel), age (28, 60, and 180 d), and temperature (20, 50, and 80 °C).

Three groups of test pieces were used for each trial from every kind of bar at the previously mentioned temperatures and ruptures at the ages of 28, 60, and 180 d, for each group. Therefore, the bonding progress of the concrete bars was tested over a sufficiently long period to analyse the increase in reinforcement for maximum compressive stress.

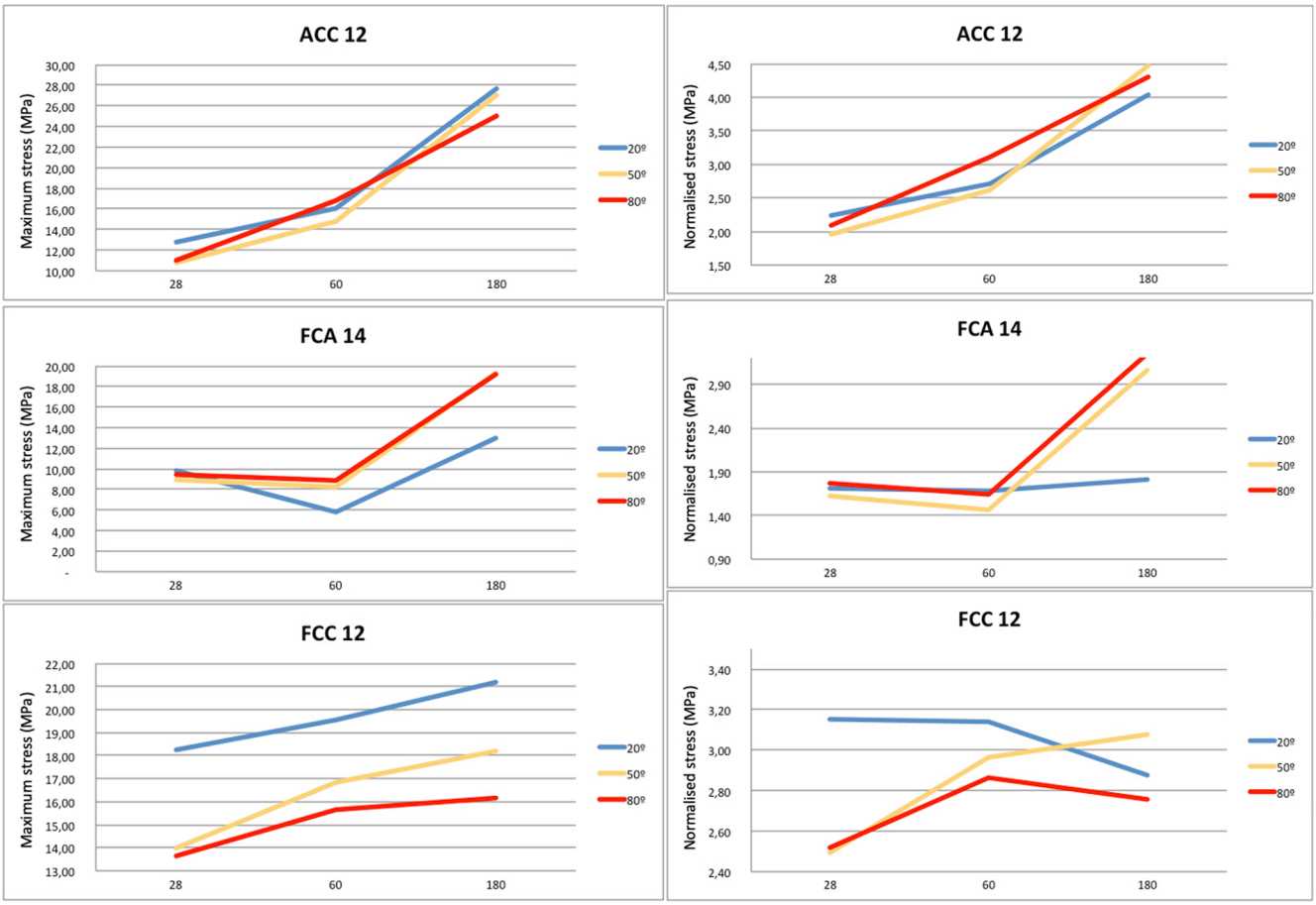

Fig. 5. Evolution of maximum stress (left) and characteristic (right) reached during the test at various sample temperatures depending on the days and climate.

Furthermore, the effect of weather on reinforced concrete was studied for a sufficient duration.

To determine the influence on bonding and compressive stress of the concrete and its effects at high temperatures, stress compression tests were conducted for each mixture of concrete.

The differences between the results on ruptures by pullout at temperatures between 20 and 50 °C are not significant [11,29]. Therefore, to compare the results of this study, a humidity variable was included in the samples at 20 °C, inducing moisture saturation.

The absence of studies on the influence of moisture on the bonding of CFRP bars is representative, even without being the main objective of this study, it is essential to know the degree of coverage that can be reached. Therefore, the samples of the pullout of each type studied, and of all ages (28, 60, and 180 d), were kept on the curing chamber with moisture-saturated samples, against those which were 50 and 80 °C, completely dry without any moisture inside.

3. Materials

The concrete used in this study was HA-30/B/20/I, made with CEM I 52, 5 R from CEMEX, sand, limestone, and superplasticiser (Sika Viscocrete 3425).

The steel bars were B 500 SD of 12 mm diameter made by Corrugados Azpeitia. The nomenclature used in this research for these bars is ACC12.

There are two types of CFRP bars: corrugated and sanded. These were selected because they are the most used and commonly available bars.

CFRP ribbed bars were made of a vinyl-ester polymeric matrix reinforced with carbon fibres. The diameter was 12 mm with an applied nomenclature FCC12 bar in this study. The manufacturer was Marshall Composites Technologies LLC.

CFRP-sanded bars were made of a vinyl-ester polymeric matrix reinforced with carbon fibres, and the bonding was achieved by silica sand coating. The diameter was 14 mm the manufacturer was Pulltrall Inc.

4. Results

Tables 1, 2, and 3 display the compressive stress in concrete (with steel bars, sand CFRP, and ribbed CFRP, respectively) at the maximum and normalised stresses of every test piece, the displacement of every endpoint, and the outcome of the batch.

In addition to the obtained data about the rupture, a column was included for each test piece with its kind of rupture, according to:

PO: A rupture that occurs after the wedging or friction between the bar and concrete fades.

RA: A rupture that occurs due to the bonding rupture between the ground geometry and bar nucleus.

RC: This rupture is a mix of PO and RA with partial bonding or wedging, but with damage to other parts of the bar. It occurs in corrugated CFRP bars, in which some corrugates endure the pressure, while others are cut.

The characterisation of rupture was completed with the pictures taken from the bars, concrete, and test pieces. Fig. 1, Fig. 2, Fig. 3., Fig. 4.

The graphics shown in Fig. 5 link the characteristic and maximum stresses for 28, 60, and 180 d, as well as display the evolution at each temperature.

Figure 6 shows the development of normalised and maximum

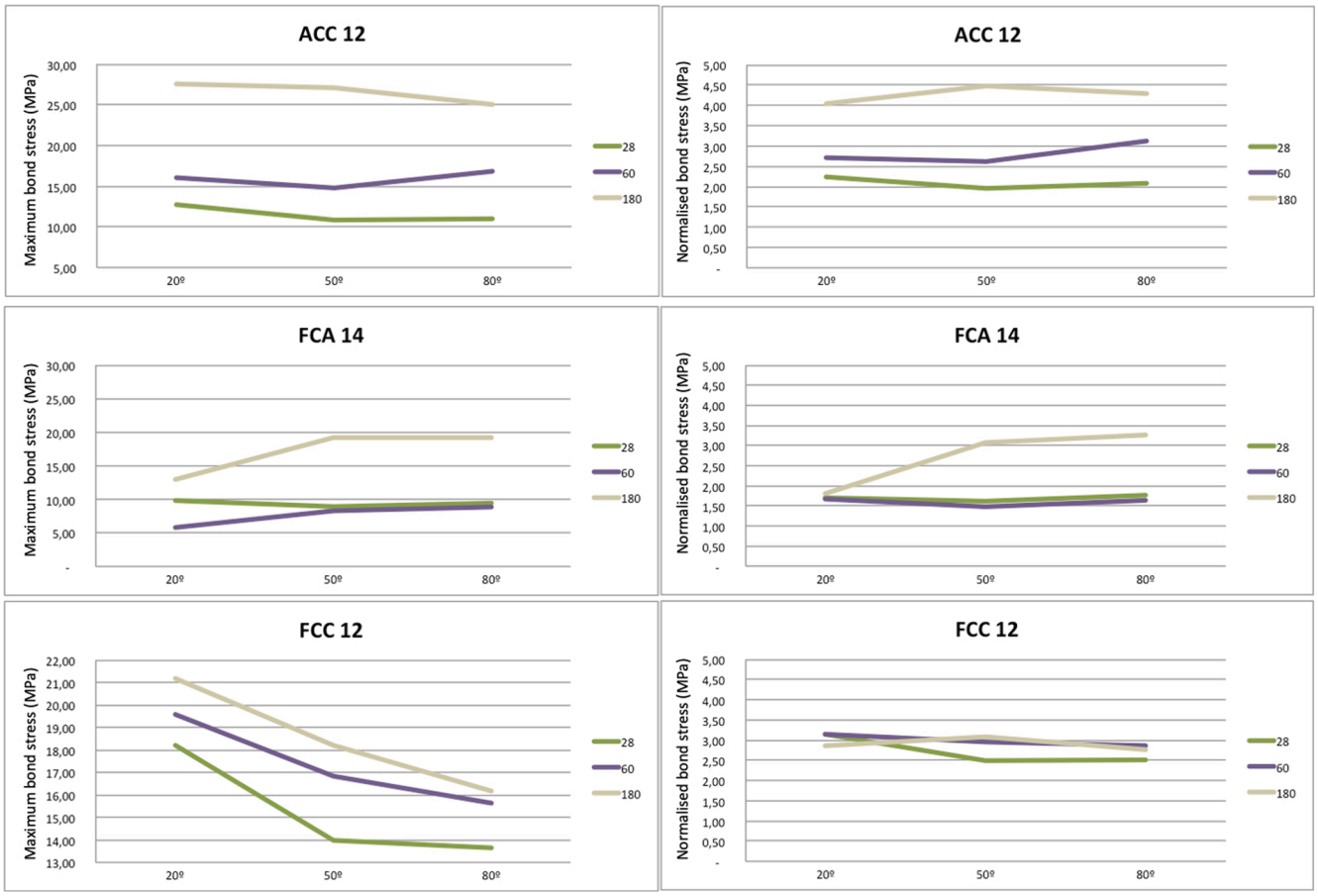

Fig. 6. Evolution of maximum stress (left) and characteristic (right) reached depending on the time period at each temperature.

stresses during the established weather conditions.

Figure 7 shows the relationship between the displacement of stressed endpoint and that of non-stressed endpoint on ribbed CFRP bars according to the age trials.

4.1. Additional testing

Four complementary tests were conducted (concrete compressive stress, optical microscopy, SEM, and AFM). The behaviour of different bars was analysed using the data obtained from these tests.

4.2. Concrete compressive stress

The development of concrete compressive stress with temperature and age was analysed. As shown in Fig. 8, the influence of high temperatures on the concrete compressive stress was directly correlated to the duration of climatic conditions of the sample, showing a decrease of approximately 28% when the samples were placed at 80 °C for 180 days. (Fig. 9. Fig. 10).

4.3. Optical microscopy

Two test pieces were analysed, one from each type of the CFRP bar regardless of the temperature and climatic conditions. These test pieces were subjected to the same climatic conditions as those used for the pullout, without being processed by pullout.

4.4. Scanning electron microscopy (SEM)

The images which suffered stress from the pullout method and those subjected to climatic conditions were taken from the bars that were used as test pieces in the pullout. The cross-sectional areas of the pieces were observed through an electron microscope. This technique reveals the behaviour of fibres and polymeric matrix, as shown in the images (Fig. 11) obtained. Here, two sanded test pieces were used: 14, 60, and 80 d old at 20, 50, and 80 °C, respectively.

4.5. *Atomic force* microscopy *(AFM)*

Atomic force microscopy (AFM) was used and detect nano-Newton forces. It consisted of a catheter that quarterly surveyed the test piece by tracking its surface from a cross-section of the CFRP bar.

5. Discussion

5.1. Influence of high temperatures on sanded CFRP

The graphs of normalised and maximum bond strengths are shown in Fig. 12. These follow the criteria mentioned in previous types of bars, according to the temperature and age in various studies.

When a bond rupture occurs (Fig. 13a, b, d), the nucleus of the bar is completely visible, as shown in the concrete coating (Fig. 13c). Fig. 14 shows the initiation of bonding by the position of sand particles in the coating and stress collapsing on the interface.

The bond strengths increase by age, which implies two things: First, the deterioration and cracking on the polymeric matrix severely affects the interface rather than the core of the bar, without developing resistance to high temperatures. Second, the bond strength can be related to the significant increase in resistance to concrete compression, which offers resistance to the superficial geometry of the bar that neutralises

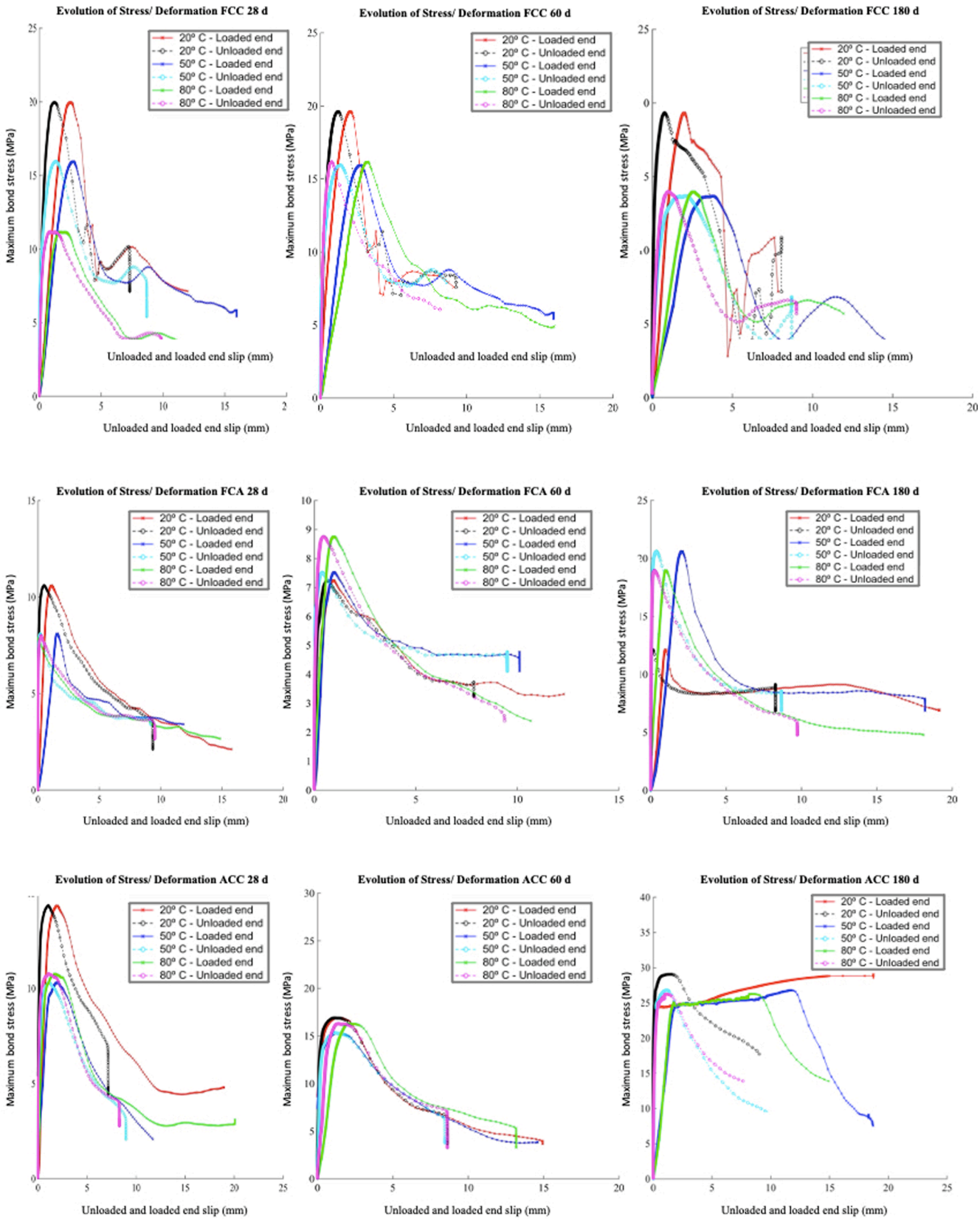

Fig. 7. Evolution of Stress/Deformation on the test samples of various CFRP and steel bars at the age of 28, 60, and 180 d at temperatures of 20, 50, and 80 °C.

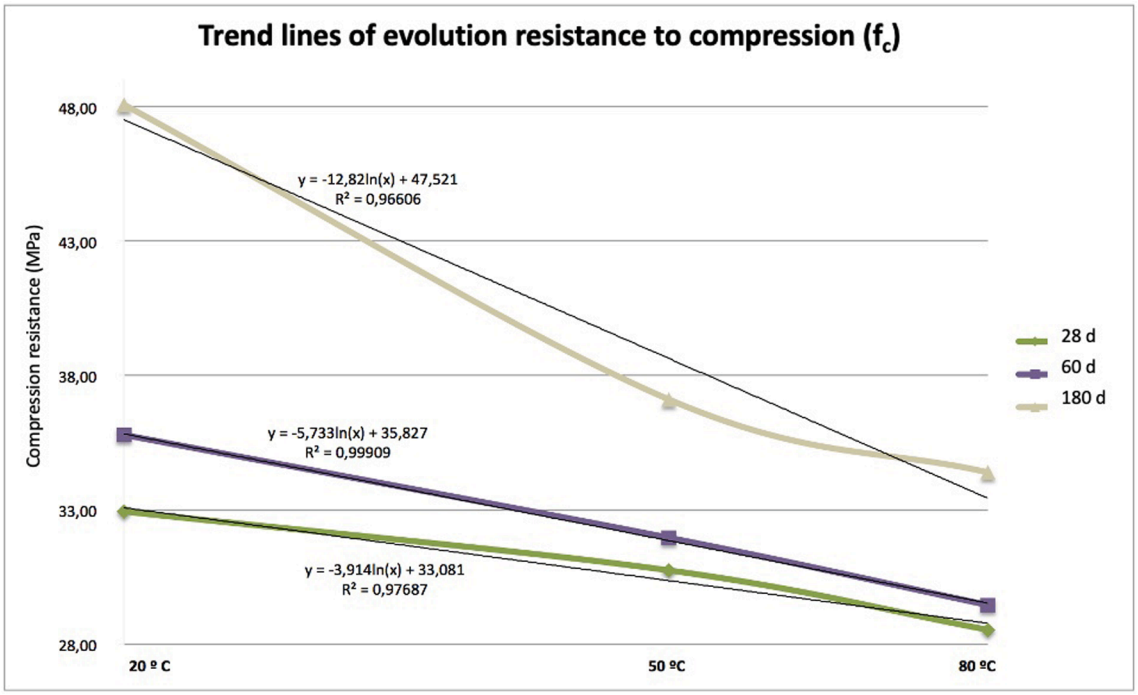

Fig. 8. Resistance to compaction tendency evolution graph of concrete depending on the age and temperature.

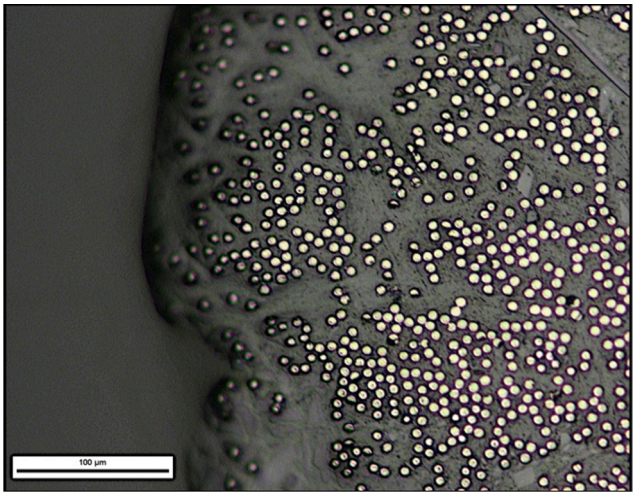

Fig. 9. Optical microscopy trial with test FCC_50/180d. Left image shows the winded side of the bar (s. 100 µm).

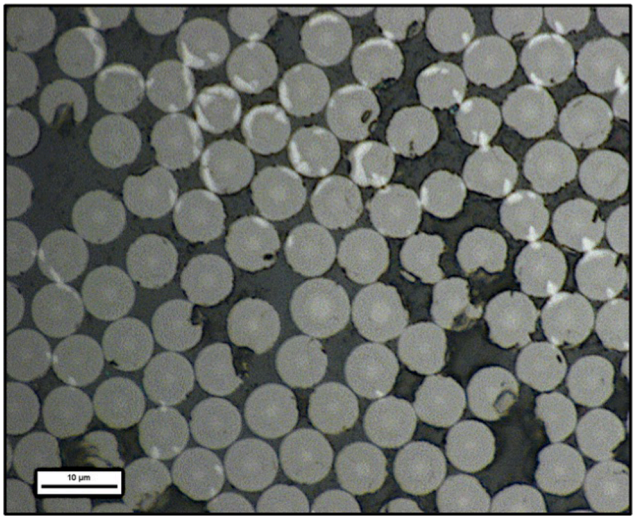

Fig. 10. Optical microscopy trial with test FCC_50/180d. Right image shows the nucleus of the bar (s. 10 µm).

the damage caused by high temperatures, combined with a complete curing of the gum from the polymeric matrix, producing a continued heating effect.

These types of ruptures and stresses occur in the parts closest to the surface of the bar and damage it. This is shown in the scanning electron microscopy (SEM) images (Fig. 15).

If we observe the inside structure of the samples by AFM, we can see the damage that has occurred due to the accumulation of stress in the polymeric matrix resin at the bar interface. As shown in the AFM image (Fig. 16), some darker places represent those areas in which the resin has been severely damaged, and brighter places represent the damage by the disappearance of resin between the fibres and the collapse that occurred.

We can conclude that the polymeric matrix resin of the inner core was not severely damaged at 80 °C in ages less than 60 d; however, some noticeable damage occurred at 180 d and 80 °C. Nevertheless, the resin at the interface showed damage at high temperatures (Fig. 15). At ages above 28 days, these damages affected the bonding by friction. Once the chemical bonding overpassed, they were compensated by the complete curing of the polymeric matrix resin and the increased resistance to compression of concrete. However, the chemical bonding provoked a brittle fracture in the bonding mechanism.

5.2. *Influence of high temperatures on ribbed CFRP bars*

The analysis of the results of normalised bond strength on CFRP bars shows a minimum development over the normalised bond strength. Due these huge differences in the compressive strength of concrete, we concluded that the normalisation cannot completely analyse the real bond phenomenon (Fig. 17).

The normalised bonding stress is between 2′52 and 3′15 MPa, with little development over climatic conditions. To determine the stress

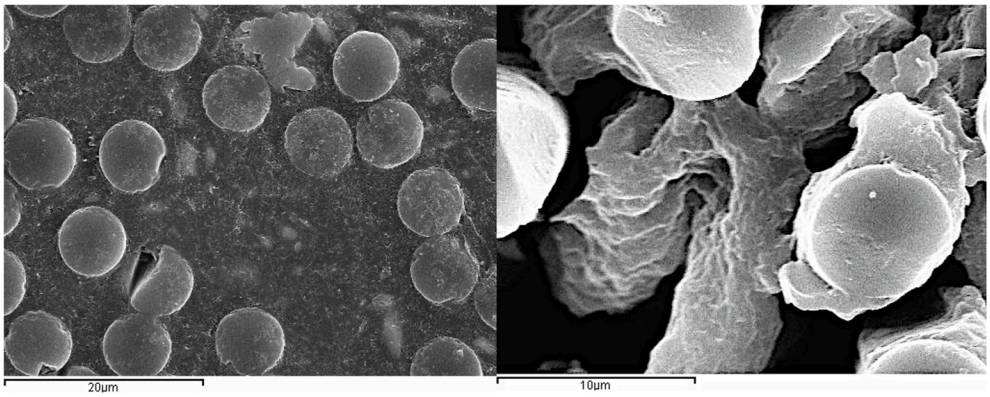

Fig. 11. (Left image) FCA_80B/180 x2500 (An interface with various polymeric matrix components); (Right image) FCA_80B/180 x5000 (A huge deterioration over the polymeric matrix at someplace on the bar).

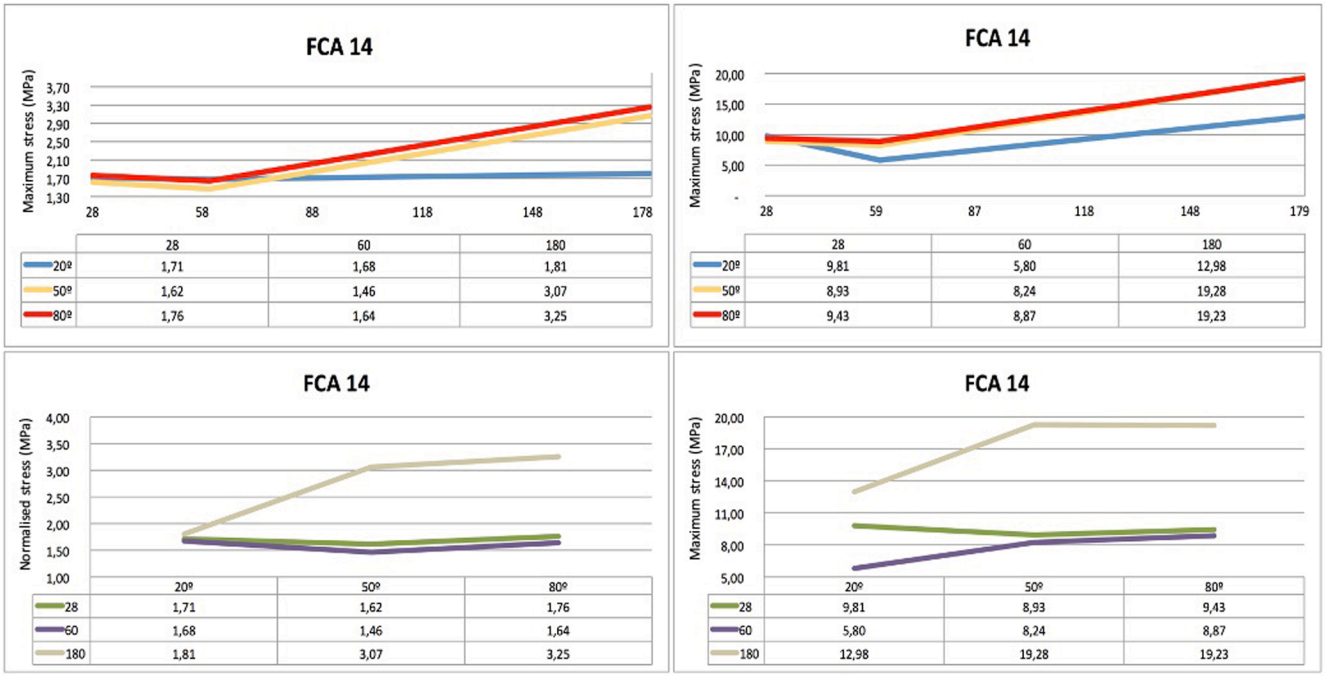

Fig. 12. Graph of maximum stress bond normalised by age and temperature, after pullout trials with sand CFRP bars.

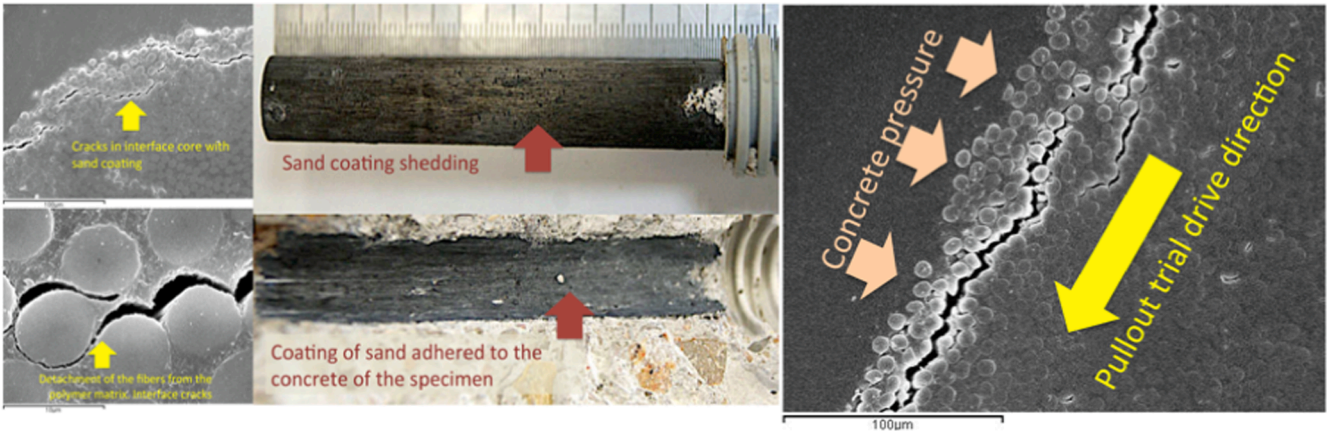

Fig. 13. a) Cracks in interface core with sand coating. b) Interface crack. c) Shedding of sand coating. d) Stress directions in a pullout test bar.

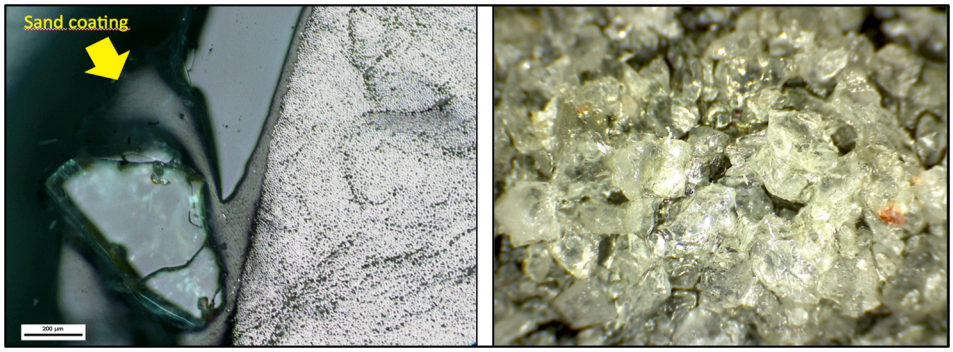

Fig. 14. Silica sand coating that forms bar geometry, which guarantees bond in the concrete bar.

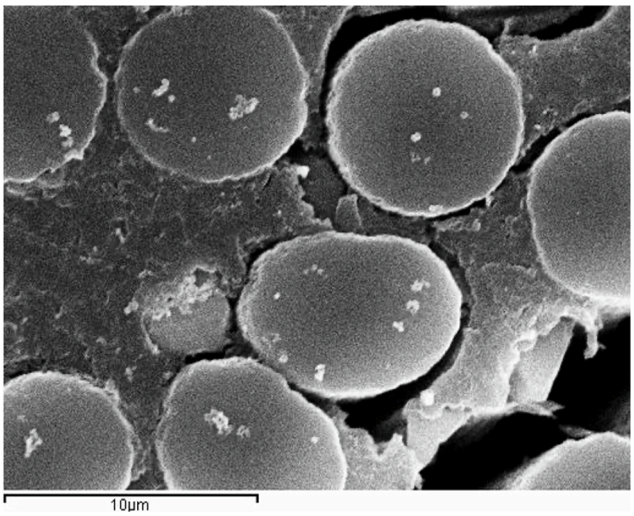

Fig. 15. Scanning electron microscopy (SEM) image of sanded CFRP.

development, data from the maximum bond strength level were added.

In ribbed CFRP bars, unlike steel bars and sanded CFRP, there is a correlation between the high temperatures and the decrease in bonding strain.

The data we obtained from 28 d of bonding strain was 18′23 MPa at 20 °C, which decreased to 13′65 MPa at 80 °C (25′12% decrease). At 60 days, the data showed 19′57 MPa at 20 °C and decreased to 15′63 MPa at 80 °C, which is a decrease of 20′13%. Finally, at 180 days, the data decreased from 21′20 MPa at 20 °C to 16′18 MPa at 80 °C, which diminishes the maximum bonding strain to 23′68%.

In summary, at every age of the study, when the temperature was higher, the bonding strain was lower.

In Figs. 18 and 19, the geometry of ribbed CFRP bars, their mechanical anchoring, and different ribbed compositions are shown.

Combined shearing appeared only at 20 °C and 28 d trial. This means that there is a relationship between the temperature and resistance to compaction of the concrete. In contrast, a generalised rupture was made by selecting corrugates over the bonding length of the bar (Fig. 20).

The corrugated bars were composed of vinyl ester resins and additional 15% SiCa and SiAl composites, whose mission was to increase the elastic modulus, facilitating a better fixation of concrete and bond resistance.

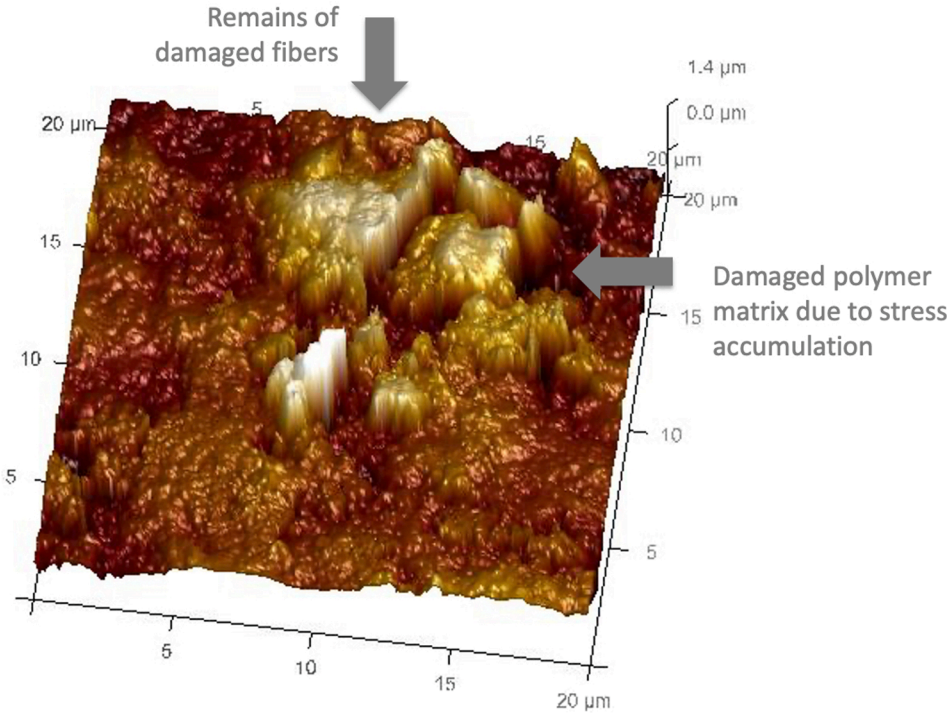

Fig. 16. Atomic force microscopy (AFM) image of sanded CFRP.

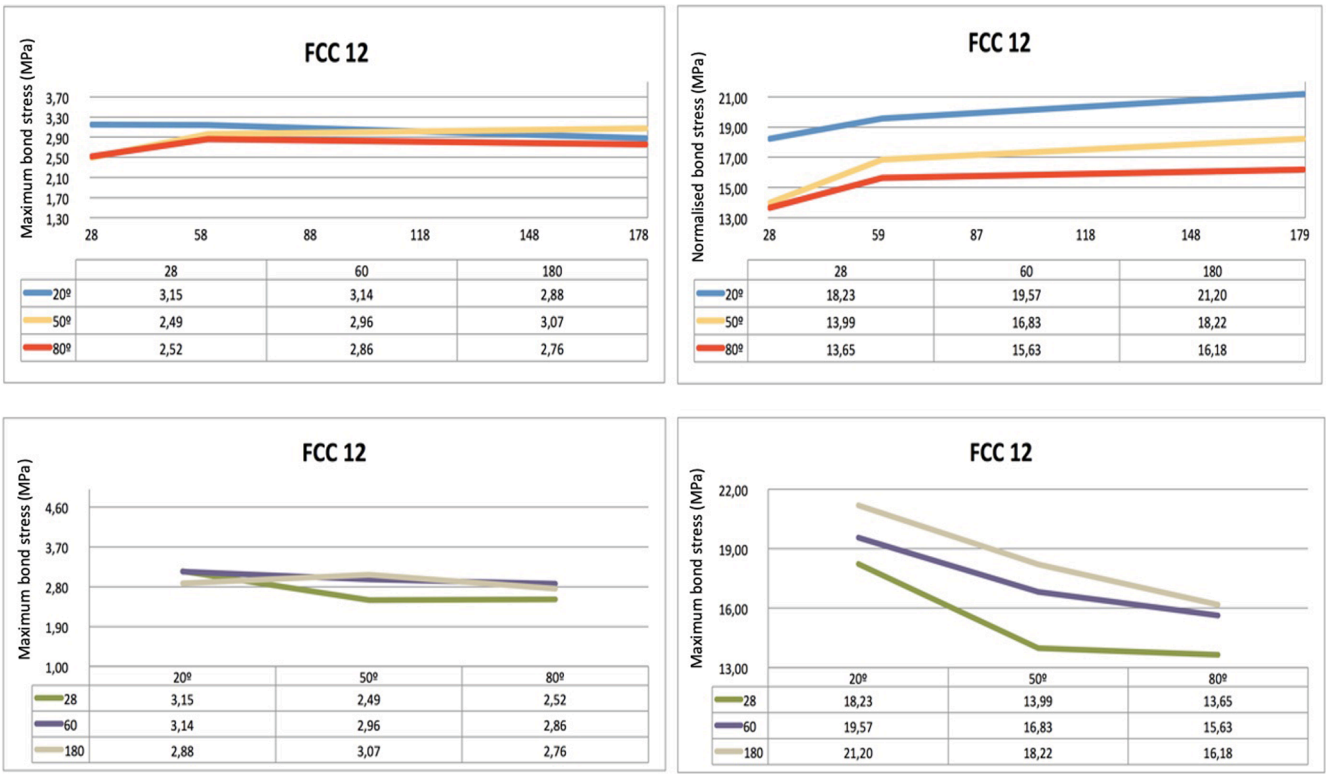

Fig. 17. Graph of maximum bond stress normalised by age and temperature, after pullout trials with sand CFRP bars.

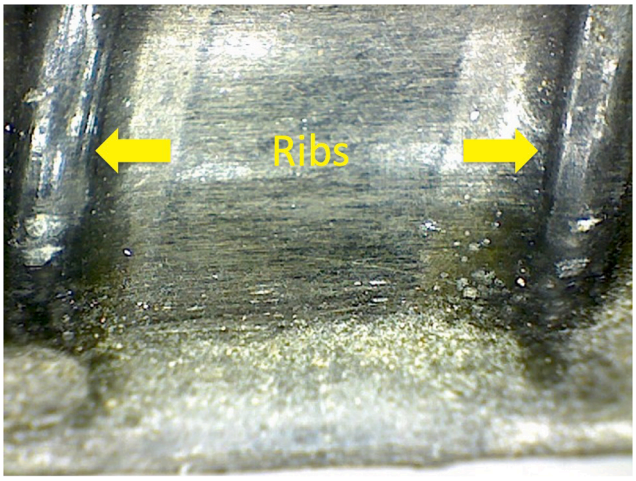

Fig. 18. Digital microscope image of a ribbed CFRP bar d12.

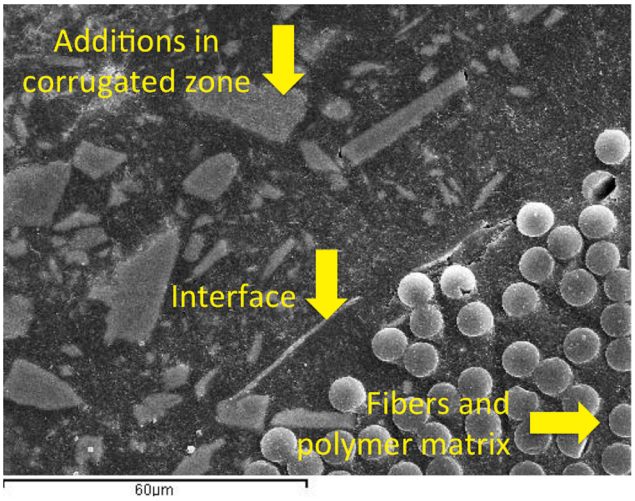

Fig. 19. SEM x1000 picture of a rib from a ribbed CFRP d12.

The high-temperature affects the stickiness of the polymeric matrix and this facilitates the maximum bond strength.

On the inside of the corrugated interface core, where the high temperatures provoke different behaviours in the elements that conform to the surface geometry and the influence of the matrix resin, as the fibres, additives, and resin, have different expansion coefficients; therefore, the internal disunity of the composite can be accelerated.

At every age of the study, when the temperature was higher, the results of the bonding stress decreased. The combined rupture only appeared at 20 °C for 28 d, which means that it is related to the temperature and compressive stress of the concrete. In contrast, the most common rupture in this research was the complete sectioning of the corrugates around the adherent length of the bar.

It is on the corrugate interface with the nucleus, where high temperatures induce different behaviours over the ground geometry. In addition to the influence of the previously mentioned matrix resin, it has different coefficients of the thermal expansion of fibres, the bonding and the resin could be accelerated to the internal unbound of the composite. As shown in Fig. 21, the deterioration of the resin is not limited to the surface of the bar and it severely affects the nucleus.

These damages occur because of the internal structure of the fibres inside the bars. An example is shown in Fig. 22. The movement of the internal polymeric matrix aligns in the form of a cross. This induces a complete non-bonding of the polymeric matrix fibres and the rupture of most of them owing to the internal distribution of the axial loads induced by the mechanical anchorage through the corrugations of the concrete, requesting traction to the bar, which causes the fibres in some

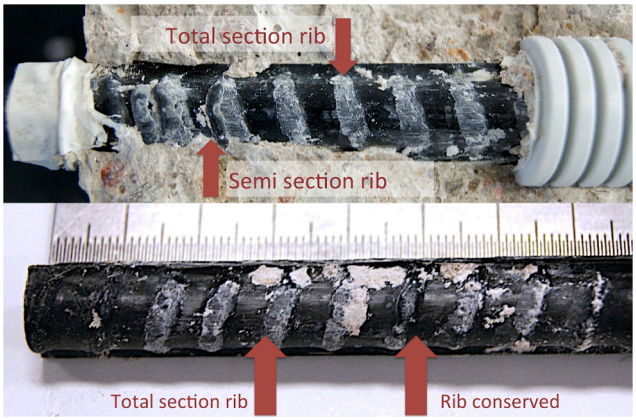

Fig. 20. Pictures taken from a test sample FCC028/20B after pullout trial, which shows conserved, section, and semi section ribs.

places to collapse.

Figure 22c shows the result of the AFM test, which was performed on a test sample of ribbed CFRP at 180 d and 80 °C to observe the surveying of the cross-sectional surface and its consequences on the climatic conditions and stress generated during the pullout. The different colours of the AFM images show the carbon fibres in a darker red deteriorated polymeric matrix.

5.3. Comparison of sanded and ribbed CFRP bars

Figure 23 shows the graphs of the rupture from the 28 d pullout sample, combined for each bar and the three temperatures analysed in this study. It was proved that ribbed CFRP bars have a higher bonding stress than other types. It was estimated that this increase is 47′06%. At 60 d, the behaviour was similar to that at 28 d, which means that at higher bonding stress and at all the temperatures studied, the bonding stress of ribbed CFRP was higher than the sanded CFRP with an estimated increase of 57–89% in the ages studied.

At 180 d the situations varied. As shown in Fig. 24, at 20 °C, the bonding stress of ribbed CFRP bars was higher than that of sanded CFRP over 45–65%. This means that, at 180 d the old behaviour observed on 28 and 60 d was followed, respectively. Although at 50 °C the stress over the sanded CFRP started to recover, unlike the ribbed CFRP, the estimated difference was 19′71%.

This tendency difference was confirmed at 80 °C when the sanded CFRP bar overpassed in the bonding corrugated by 12–14%.

The ribbed CFRP mobilised their main bonding by the mechanical anchoring of concrete corrugates, causing a huge traction over the nucleus fibres (Fig. 22a). This fact is incredibly positive for average thermic conditions because excellent traction behaviour is one of the main characteristics of carbon fibres. However, this may cause a problem when the temperatures rise, and it affects the vinyl ester resin in the nucleus and in the formation of corrugates, which facilitates the necessary bonding of the polymeric fibre/matrix.

The resistance to compaction influences the effects over both textures, but on a larger scale, they facilitate the development of the maximum bond strain in sanded CFRP bars because of the confinement effect.

6. Conclusions

1.- CFRP bars are influenced by high temperatures on their bonding behaviour, depending on the surface treatment specific from each type.

2.- The bonding stress on ribbed CFRP bars suffers a downsizing of 23–68% in extended periods of time and high temperature (180 d and 80 °C), concerning the temperature control (20 °C). Steel bars suffer a downsizing of 9′58%

3.- Sanded CFRP bars are not affected by the temperatures up to 80 °C for 180 d, reaching higher values than ribbed CFR bars at that age

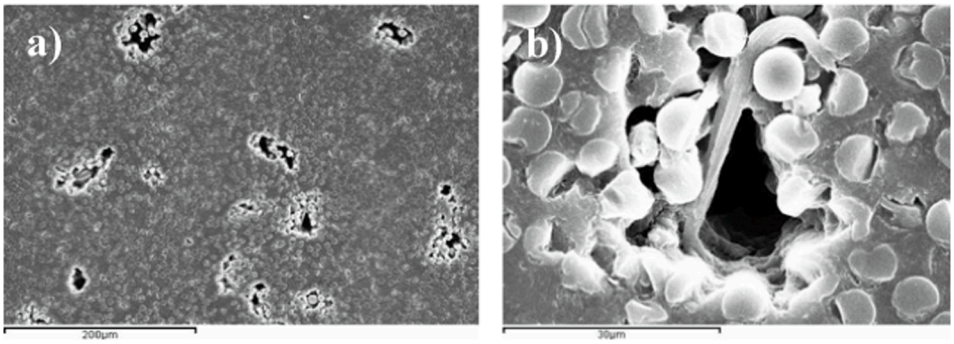

Fig. 21. a) SEM x250 image of the nucleus of FCC180/80B test bar with generalised damage over the resin. b) SEM x2000 image of the nucleus of FCC180/80B test bar with severe damage over the resin.

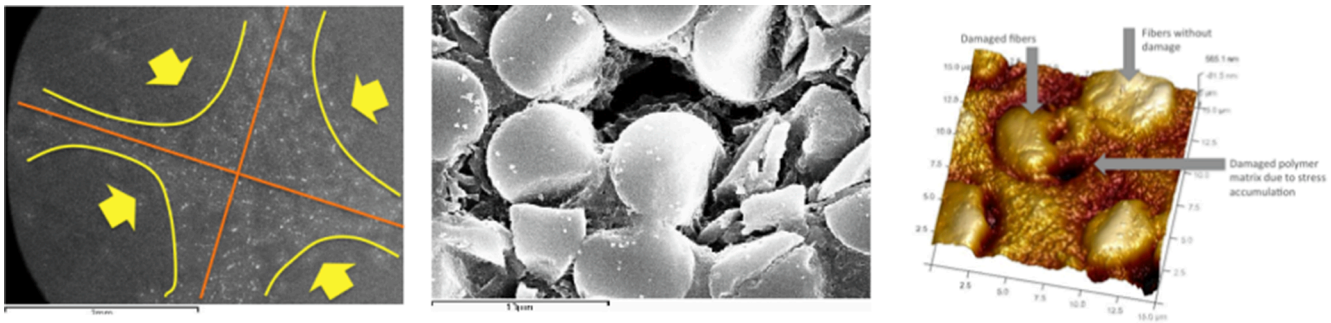

Fig. 22. a) Gathering of axial forces on the fibre nucleus of a ribbed CFRP bar. b) SEM image of the nucleus fibre collapse on FCC060/50C test bar of ribbed CFRP owing to charge alignment and deterioration of the polymeric matrix. c) AFM image of FCC180/80C test sample.

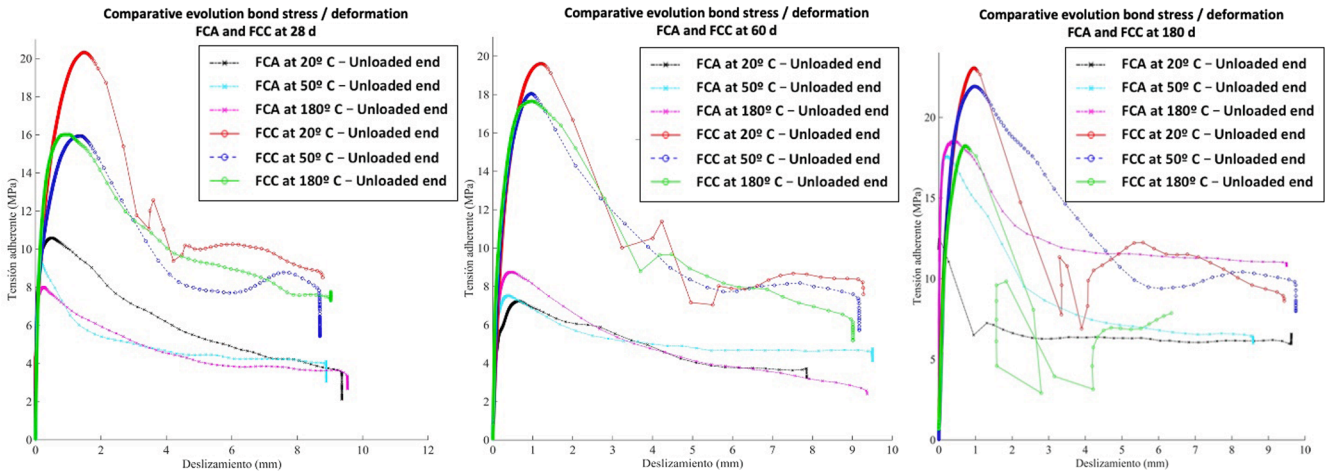

Fig. 23. Comparison of the development of stress/deformation over ribbed and sanded CFRP bars.

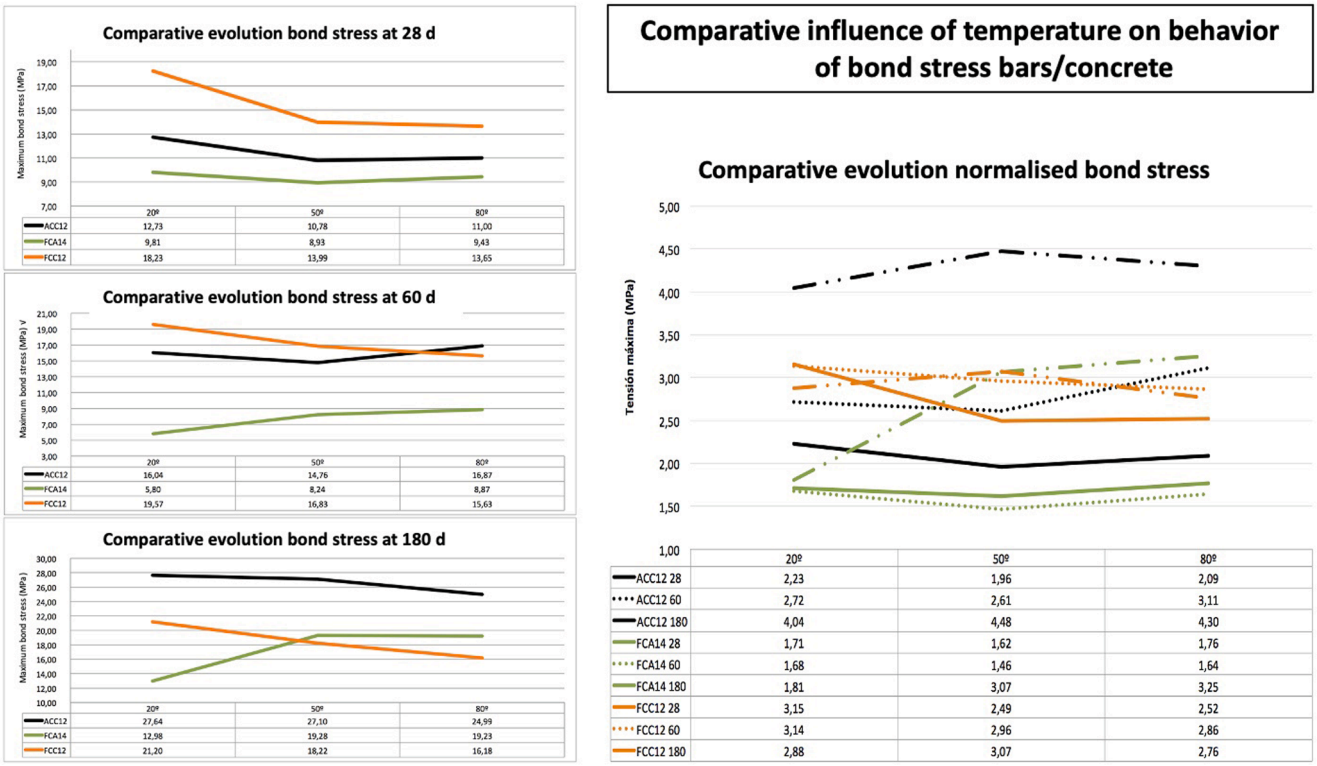

Fig. 24. Comparison of the development of stress/deformation over steel and CFRP bars (ribbed and sanded).

and temperature. These bars registered a stable behaviour from 50 to 80 °C and strains between 19′28 and 19′27 MPa, respectively, which means that temperatures till 80 °C do not affect the bonding in this type of concrete bar.

4.- Comparing the three samples of bars at 20 °C, the maximum bond strength is 18′23 MPa by ribbed CFRP bars, against 12′73 MPa from the steel bars, which is a 30′17% increase.

5.- Sanded CFRP bars are susceptible to water. In this research, it is proved that, in moisture, the bonding stress values do not increase and remain stable from the 28th day, which is related to the composition of the superficial core.

6.- The shearing on the sanded bars is more fragile than the corrugated bars, which is higher at higher temperatures, where almost instantaneously the collapse of the sanded coating occurs, followed by a complete slipping of the bar. This makes them less suitable for structural use because stiffness decreases the safety factors.

CRediT authorship contribution statement

Fernando Cos-Gayón López: Conceptualization, Methodology, Software, Investigation, Writing – original draft, Writing - review & editing. **Javier Benlloch Marco:** Conceptualization, Methodology, Software, Investigation, Writing – original draft, Writing - review & editing. **Víctor Calvet Rodríguez:** Conceptualization, Methodology, Software, Investigation, Writing – original draft, Writing - review & editing.

Declaration of Competing Interest

The authors declare that they have no known competing financial

interests or personal relationships that could have appeared to influence the work reported in this paper.

Acknowledgments

The authors would like to thank the manufacturer of the sanded CFRP V Rod (Pultrall Inc., Thetford Mines, Quebec, Canada) and ribbed CFRP C-bar (Marshall Composite Technologies LLC, Salem, Oregon, USA) for providing the CFRP bars. Funding for open access charge: CRUE-Polytechnic University of Valencia.

References

[1] S. Faza, Bending and Bond Behavior and Design of Concrete Beams Reinforced with Fiber Reinforced Plastic Rebars, West Virginia State University, 1991.
[2] A. Castañeda-Valdez, M. Rodriguez-Rodriguez, Las pérdidas económicas causadas por el fenómeno de la corrosión atmosférica del acero de refuerzo embebido en el hormigón armado, CENIC Ciencias Químicas 45 (2014) 52–59.
[3] L.C. Hollaway, A review of the present and future of FRP composites in the civil infrastructure with reference to their important in-service properties, Constr. Build. Mater. 24 (12) (2010) 2419–2445, https://doi.org/10.1016/j.conbuildmat.2010.04.062.
[4] C.E. Bakis, in: Fiber-Reinforced-Plastic (FRP) Reinforcement for Concrete Structures, Elsevier, 1993, pp. 13–58, https://doi.org/10.1016/B978-0-444-89689-6.50006-9.
[5] Z.P. Achillides ZP. Bond behaviour of FRP bars to concrete. Roc., 3rd Int. Symp. On Non-Metallic (FRP) Reinforcement for Concrete Structures 1997; 341-348. Japan Concrete Society.
[6] M.M. Al-Zahrani, S.U. Al-Dulaijan, A. Nanni, C.E. Bakis, T.E. Boothby, Evaluation of bond using FRP rods with axisymmetric deformations, Constr. Build. Mater. 13 (6) (1999) 299–309, https://doi.org/10.1016/S0950-0618(99)00038-0.
[7] M. Baena, L. Torres, A. Turon, C. Barris, Experimental study of bond behaviour between concrete and FRP bars using a pull-out test, Compos. Part B-Eng 40 (8) (2009) 784–797, https://doi.org/10.1016/j.compositesb:2009.07.003.
[8] B. Benmokrane, E. El-Salakawy, S.E. El-Gamal, S. Goulet, Construction and Testing of Canada's First Concrete Bridge Deck Totally Reinforced with Glass FRP Bars, J. Bridge Eng. 12 (5) (2007) 632–645, https://doi.org/10.1061/(ASCE)1084-0702(2007)12:5(632).
[9] E.A. Byars, P. Waldron, V. Dejke, S. Demis. Durability of FRP in concrete deterioration mechanisms. FRP Compos. Civ. Eng. 2 2001 1517–1525. ISBN: 0-08-043945-4.
[10] K.K. Chang, in: Composites, ASM International, 2001, pp. 41–45, https://doi.org/10.31399/asm.hb.v21.a0009242.
[11] J.F. Davalos, Y. Chen, I. Ray, Effect of FRP bar degradation on interface bond with high strength concrete, Cem. Concr. Compos. 30 (8) (2008) 722–730, https://doi.org/10.1016/j.cemconcomp.2008.05.006.
[12] A.D. Edwards, P.J. Yannopoulos, Local bond stress-slip relationship under repeated loading, Mag. Concr. Res. 30 (103) (1978) 62–72, https://doi.org/10.1680/macr.1978.30.103.62.
[13] R.F. Gibson, Principles of Composite Material Mechanics, fourth ed., CRC Press, 2016.
[14] L.J. Malvar, N.R. Joshi, B. Ja, T. Novinson, Environmental effects on the short-term bond of carbon fiber-reinforced polymer CFRP composites, J. Compos. Constr. 7 (1) (2003) 58–63, https://doi.org/10.1061/(ASCE)1090-0268(2003)7:1(58).
[15] A. Nanni, Guide and Specifications for the Use of Composites in Concrete and Masonry Construction in North America, in: Proceedings of the International Workshop Composites in Construction: A Reality, 2001, pp. 9–18.
[16] M.M. Schwartz, Composite Materials Handbook, second ed., McGraw-Hill, New York, 1992.
[17] R. Tepfers, Bond clause proposal for FRP-bars/rods in concrete based on CEB/FIP Model Code 90. Part 1: design bond stress for FRP reinforcing bars, Struct. Concr. 7 (2) (2006) 47–55.
[18] Y.C. Wang, P.M.H. Wong, V. Kodur, An experimental study of the mechanical properties of fibre reinforced polymer (FRP) and steel reinforcing bars at elevated temperatures, Compos. Struct. 80 (1) (2007) 131–140.
[19] W.M. Yuan, Buckling analysis of concrete-filled FRP tubes, Int. J. Struct. Stab. Dyn. 1 (3) (2001) 367–383.
[20] H.M. Mohamed, A.H. Ali, B. Benmokrane. Behavior of circular concrete member reinforced with carbon-FRP bars and spirals under shear. J. Compos. Constr. 21(2) 2017 04016090-1/12. https://doi.org/10.1061/(ASCE)CC.1943-5614.000746.
[21] E.A. Ahmed, E.F. El-Salakawy, B. Benmokrane. Shear performance of RC bridge girders reinforced with carbon FRP stirrups. ASCE J. Bridge Eng. 15(1) 2010 44-54. https://doi.org/(ASCE)BE.1943-5592.000035.
[22] A.K. El-Sayed, E.F. El-Salakawy, B. Benmokrane. Mechanical and structural characterization of new carbon FRP stirrups for concrete members, ASCE J. Compos. Constr. 11(4) 2007 352-362. https://doi.org/(ASCE)1090-0268(2007)11:4(352).
[23] H.A. Mesbah, R. Benzaid, B. Benmokrane, Evaluation of bond strength of FRP reinforcing rods in concrete and FE modelling, Int. J. Civ. Eng. Constr. Sci. 4 (3) (2017) 21–41.
[24] B. Benmokrane, B. Zhang, K. Laoubi, B. Tighiouart, I. Lord. Mechanical and bond properties of new generation of carbon fibre reinforced polymer reinforcing bars for concrete structures, Can. J. Civ. Eng. 29 2002 338-343. https://doi.org/10.1139/L02-013.
[25] D. Moon, U. Ebead, B. Benmokrane, Effective surface deformation height and bond rigidity of FRP reinforcing bars with ribs, Polym. Polym. Compos. 17 (3) (2009) 161–171, https://doi.org/10.1177/096739110901700305.
[26] M.A. Aiello, M. Leone, M. Pecce, Bond performances of FRP rebars-reinforced concrete, ASCE J. Mater. Civ. Eng. 19 (3) (1997) 203–210, https://doi.org/10.1061/(ASCE)0899-1561(2007)19:3(205).
[27] V. Calvet, M. Valcuende, J. Benlloch, J. Cánoves. Influence of moderate temperatures on the bond between carbon fibre reinforced polymer bars (CFRP) and concrete, Constr. Build. Mater. 94 2015 589-604. https://doi.org/ j.conbuildmat.2015.07.053.
[28] R.J.A. Hamad, M.A. Megat-Johari, R.H. Haddad. Mechanical properties and bond characteristics of different fiber reinforced polymer rebars at elevated temperatures, Constr. Build. Mater. 142 2017 521-535. https://doi.org/ j.conbuildmat.2017.03.113.
[29] Z. Achillides, K. Pilakoutas, Bond behavior of fiber reinforced polymer bars under direct pullout conditions, J. Compos. Constr. 8 (2) (2004) 173–181, https://doi.org/10.1061/(ASCE)1090-0268(2004)8:2(173).
[30] B. Tighiouart, B. Benmokrane, D. Gao, Investigation of bond in concrete member with fibre reinforced polymer (FRP) bars, Constr. Build. Mater. 12 (8) (1998) 453–462, https://doi.org/10.1016/S0950-0618(98)00027-0.
[31] B. Benmokrane, B. Tighiouart, O. Chaallal, Bond Strength and load distribution of composite GFRP Reinforcing Bars in Concrete, ACI Mater. J. 93 (3) (1996) 246–253.
[32] S. Islam, H.M. Afefy, K. Sennah, H. Azimi. Bond characteristics of straight and headed-end, ribbed-surface, GFRP bars embedded in high-strength concrete, Constr. Build. Mater. 83 2015 283-298. https://doi.org/j.conbuildmat.2015.03.025.
[33] A. Hadhood, H.M. Mohamed, B. Benmokrane. Strength of circular HSC columns reinforced internally with carbon-fiber-reinforced polymer bars under axial and eccentric loads, Constr. Build. Mater. 141 2017 366-378. https://doi.org/10.106/j.conbuildmat.2017.02.117.
[34] L.C. Bank, M. Puterman, A. Katz, The effect of material degradation on bond properties of fiber reinforced plastic reinforcing bars in concrete, ACI Mater. J. (1998) 232–243.
[35] M.M. Rafi, A. Nadjai, F. Ali, D. Talamona, Aspects of behaviour of CFRP reinforced concrete beams in bending, Constr. Build. Mater. 22 (3) (2008) 277–285, https://doi.org/10.1016/j.conbuildmat.2006.08.014.
[36] E. Nigro, A. Bilotta, G. Cefarelli, G. Manfredi, E. Cosenza, Performance under Fire situations of concrete members reinforced with FRP rods: bond models and design Nomograms, J. Compos. Constr. 16 (4) (2012) 395–406, https://doi.org/10.1061/(ASCE)CC.1943-5614.0000279.
[37] A. Katz, N. Berman, L.C. Bank, Effect of high temperature on bond strength of FRP rebars, J. Compos. Constr 3 (2) (1999) 73–81, https://doi.org/10.1061/(ASCE)1090-0268(1999)3:2(73).
[38] A. Katz. Effect of cyclic loading and elevated temperature on the bond properties of FRP rebars. Int. Conference on the Durability of Fiber Reinforced Polymere (FRP) for Construction, Canada, 1998. 403–413.
[39] M. Saafi. Effect of fire on FRP reinforced concrete members, Compos. Struct. 58(1) 2002 11-20. https://doi.org/S0263-8223(02)00045-4.
[40] E.B. Lublóy, Bond of CFRP wires under elevated temperature, in: Proceedings of the International Symposium on Bond Behaviour of FRP in Structures (BBFS), 2005, pp. 163–168.
[41] L.A. Bisby, M.F. Green, V.K.R. Kodur, Kodur VKR Response to Fire of Concrete Structures that Incorporate FRP, Prog. Struct. Eng. Mater. 7 (3) (2005) 136–149, https://doi.org/10.1002/(ISSN)1528-271610.1002/pse.v7:310.1002/pse.198.
[42] R. Masmoudi, A. Masmoudi, M.B. Ouezdou, A. Daoud. Long-term bond performance of GFRP bars in concrete under temperature ranging from 20°C to 80°C, Constr. Build. Mater. 25(2) 2011 486-493. https://doi.org/ 10.1016/j.conbuildmat.2009.12.040.
[43] M.M. Rafi, A. Nadjai, F. Ali. Fire resistance of carbon FRP reinforced-concrete beams, Mag. Concr. Res. 59(4) 2007 245-255. https:/doi.org/10.1680/macr.2007.59.4.245.